Marine Environmental Research 212 (2025) 107553

Contents lists available at ScienceDirect

Marine Environmental Research

journal homepage: www.elsevier.com/locate/marenvrev

Seasonal dynamics at low trophic level and ecological interactions of microbial and plankton communities during harmful algal blooms

Yunjung Park [a], Joonyeop Lee [a], Soonmo An [b,c,*], Jaeho Cha [a,d,**]

[a] Department of Microbiology, College of Natural Sciences, Pusan National University, Busan, 46241, Republic of Korea
[b] Department of Oceanography, College of Natural Sciences, Pusan National University, Busan, 46241, Republic of Korea
[c] Marine Research Institute, Pusan National University, Busan, 46241, Republic of Korea
[d] Microbiological Resource Research Institute, College of Natural Sciences, Pusan National University, Busan, 46241, Republic of Korea

A B S T R A C T

This study investigates the seasonal dynamics of microbial and plankton communities in Tongyeong (TY) and the Bodol Sea near Yeosu (YS), South Korea, focusing on the interactions during algal blooms and their ecological implications. In May at TY, moderate chlorophyll a (Chl-a) and high copepod abundance suggest top-down control by zooplankton grazing, rather than nutrient limitation, regulates phytoplankton biomass. Microbial communities resembled those during August YS blooms, likely due to enhanced organic matter from grazing. By late summer, reduced nutrients favored *Dinoflagellata* and *Ochrophyta* indicating weakened grazing pressure and greater microbial diversity.

In August at YS, a harmful *Cochlodinium* bloom dominated offshore waters, while diatoms prevailed nearshore. Elevated Chl-a, oversaturated oxygen, and low copepod abundance indicated disrupted trophic balance during the blooming. *Cochlodinium* correlated strongly with bacteria such as *Pseudoaltermonas* and *Vibrio*, reflecting responses to high productivity. After the bloom decline in September, *Syndiniales* (parasitic dinoflagellates) increased, suggesting predator-prey regulation of algal populations. Bacterial remineralization supported nutrient cycling, maintaining ecosystem balance.

Contrasting responses to high productivity were observed: TY exhibited strong top-down control without biomass accumulation, whereas YS experienced significant biomass buildup during the bloom. Despite these differences, the microbial communities in both systems were similar and reflected the degree of productivity more accurately than the primary producers themselves. Overall, these results highlight the complex interactions among primary producers, grazers, and microbes, emphasizing the critical role of trophic dynamics in shaping coastal bloom events.

1. Introduction

Pelagic ecosystems are regulated by two mechanisms; top-down (predator-driven) and bottom-up (resource-driven) controls (Frank et al., 2007; Vinueza et al., 2014). Top-down mechanisms involve predators, particularly zooplankton, that regulate phytoplankton, thereby influencing community structure at lower trophic levels. In contrast, bottom-up mechanisms are driven by nutrient availability and primary production, which govern the abundance and composition of phytoplankton, and subsequently affect herbivore and higher trophic level populations. While both mechanisms are critical in regulating pelagic ecosystems (Banse, 2007, 2013; Frank et al., 2007; Rodríguez-Gálvez et al., 2023; Sommer, 2000), much research has focused predominantly on bottom-up processes, often neglecting the interactive effects of both mechanisms (Antell and Saupe, 2021). However, some studies suggest that zooplankton grazing may have a stronger influence on phytoplankton biomass than nutrient availability (Calbet and Landry, 2004; Goericke, 2002; Metaxas and Scheibling, 1996; Odate and Imai, 2003). The complexity of marine ecosystems, combined with numerous interacting environmental factors, has made it difficult to obtain direct evidence of top-down effects in natural field conditions (Odate and Imai, 2003; Stenseth et al., 2006). Nevertheless, integrated studies that examine how top-down and bottom-up mechanisms interact in natural ecosystems are essential for a comprehensive understanding of pelagic marine dynamics.

At lower trophic levels, phytoplankton, zooplankton, and microbes are important groups in maintaining ecosystem function. Phytoplankton provides the chemical energy that sustains marine food webs, whereas heterotrophic bacteria decompose organic matter and recycle nutrients, often stimulating phytoplankton growth through ammonium remineralization or by providing vitamins (Amin et al., 2015; Cho et al., 2015; Gonzalez and Bashan, 2000; Hernandez et al., 2009). Zooplankton primarily feed on phytoplankton, helping to regulate their populations and preventing harmful blooms that can disrupt ecosystem balance (Belfiore

* Corresponding author. Department of Oceanography, College of Natural Sciences, Pusan National University, Busan, 46241, Republic of Korea.
** Corresponding author. Department of Microbiology, College of Natural Sciences, Pusan National University, Busan, 46241, Republic of Korea.
E-mail addresses: sman@pusan.ac.kr (S. An), jhcha@pusan.ac.kr (J. Cha).

https://doi.org/10.1016/j.marenvres.2025.107553
Received 3 April 2025; Received in revised form 25 August 2025; Accepted 14 September 2025
Available online 18 September 2025

et al., 2021; Ekvall et al., 2014). Additionally, zooplankton grazing facilitates nutrient cycling by converting organic matter into forms more accessible to other marine organisms through the excretion of dissolved inorganic nitrogen (Saba et al., 2009; Sailley et al., 2015). However, the dynamics of these communities are highly sensitive to environmental changes. For example, fluctuations in nutrient levels, temperature, and light intensity can lead to rapid shifts in phytoplankton populations, potentially causing ecological imbalances like harmful algal blooms (HABs) (Morabito et al., 2018; Saito et al., 2006). While not all algal blooms are harmful, blooms of toxin-producing species can severely impact marine life and pose significant threats to marine ecosystems (Grattan et al., 2016; Van Dolah, 2000). Understanding how environmental factors shape these dynamics is essential for predicting and managing ecological disruptions like HABs.

The interactions between these communities further complicate marine ecosystem dynamics. In certain regions, top-down predators are considered key regulators of phytoplankton blooms (Rodríguez-Gálvez et al., 2023). Phytoplankton blooms can also affect microbial community structures, driving shifts in bacterial populations and creating tightly coupled relationships between microbial dynamics and phytoplankton activity (Buchan et al., 2014; Riemann et al., 2000). Significant correlations between bacterial and phytoplankton communities have been observed in regions such as the shelf waters off the Ría de Vigo and the Eastern North Atlantic Ocean (Costas-Selas et al., 2022; Joglar et al., 2021). Moreover, blooms of high-toxin-producing species often reduce bacterial diversity (Sison-Mangus et al., 2016). This suggests that specific algal species identify influences bacterial communities more than the bloom magnitude. Despite these findings, the detailed interactions between phytoplankton, zooplankton, and microbial communities remain incompletely understood in marine ecosystems.

In the Bodol Sea near Yeosu (YS) and Tongyeong (TY) in the South Sea of Korea, coastal eutrophication, driven by nutrient inflow from nearby fish farms, has been observed (Lee et al., 2017; Kang et al., 2003). This nutrient enrichment, combined with sluggish seawater circulation, often creates favorable conditions for algal blooms, which can significantly impact the local aquaculture industry (Lee and Kim, 2008). Previous studies have shown that blooms of *Cochlodinium polykrikoides* near TY are associated with distinct microbial communities, differing from those linked with other algal species such as *Alexandrium*, *Chaetoceros,* or *Chattonella* (Cui et al., 2020). While algal blooms are common in these regions, they do not occur annually, and their severity, species composition, and duration can vary depending on environmental and geographical factors. Comparative studies between these two locations could provide valuable insights into the complex interactions among these communities, enhancing our understanding of how environmental imbalances, such as algal blooms, impact marine ecosystems.

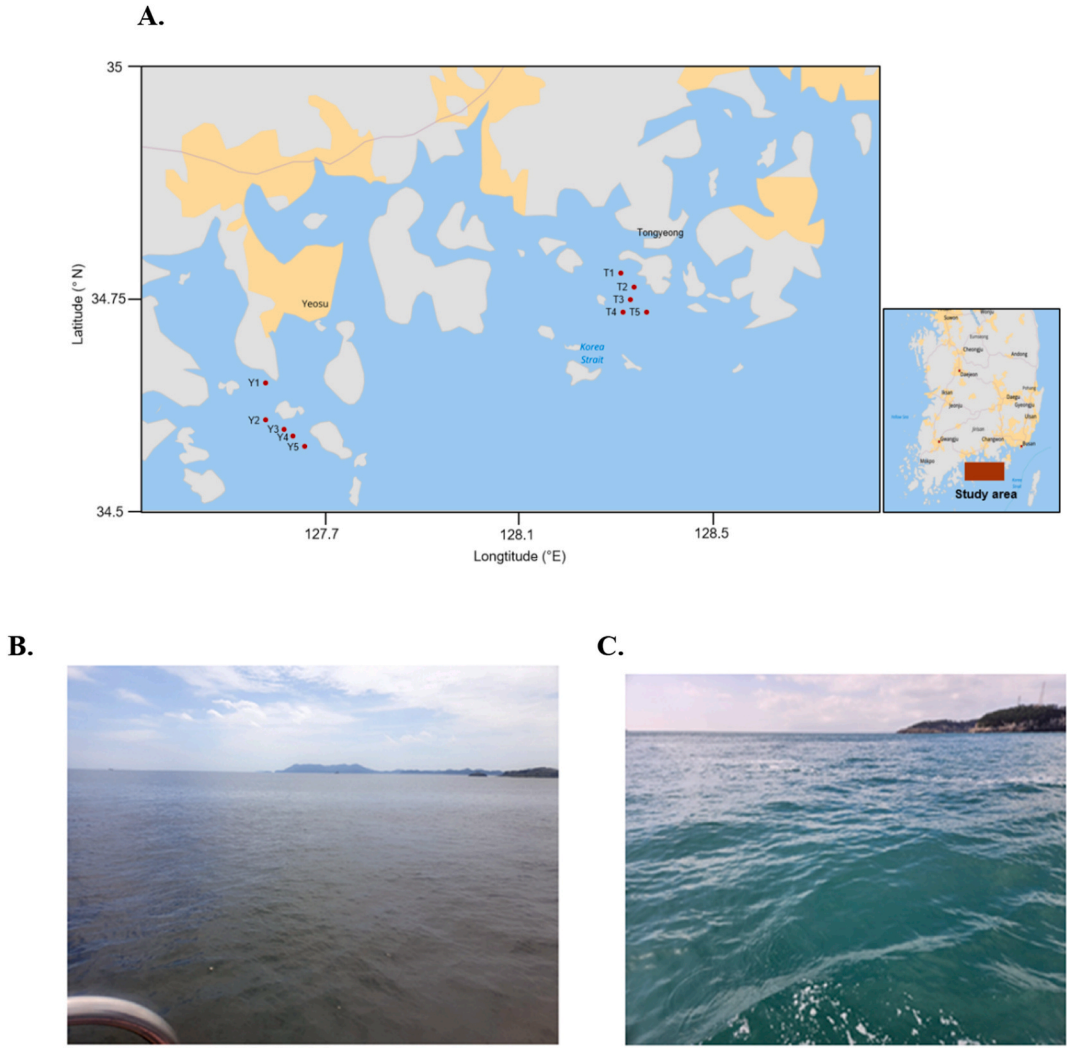

Fig. 1. This map illustrates the sampling sites along the Bodol sea coast in the Yeosu (YS) and Tongyeong (TY) areas (**A**). The color of seawater on the Bodol sea coast of YS reveals a dark red color during a red tide event in August (**B**), while normal seawater is shown for comparison after the disappearance of the red tide in September of YS (**C**). (For interpretation of the references to color in this figure legend, the reader is referred to the Web version of this article.)

In this study, we selected two sampling sites, TY and YS, to examine seasonal variations in zooplankton, phytoplankton, and bacterial communities. By analyzing water samples collected during blooms and non-bloom periods, we aimed to elucidate how environmental changes affect microbial and plankton community composition. We utilized molecular techniques, including high-throughput sequencing and quantitative PCR (qPCR), to assess the diversity and abundance of bacteria, phytoplankton, and zooplankton. Furthermore, we explored the relationships between microbial and plankton communities in relation to environmental factors such as seasonality, algal blooms, and nutrient concentrations.

2. Materials and methods

2.1. Sampling sites and collection

Water samples were collected at five sites each in Yeosu (YS) and Tongyeong (TY), South Korea (Fig. 1). TY was sampled in May, August, and September 2022; YS was sampled twice (August and September 2022) at fixed coordinates. Surface water samples within 0.1 m depth were collected from each site using 2 L water collection bottles and transported directly to the laboratory at Pusan National University, South Korea. Seawater (400 mL) was vacuum-filtered (0.2 μm) for DNA extraction (stored at −80 °C); filtrates were kept at −20 °C for nutrient analysis.

2.2. Measurement of environmental parameters

To assess environmental conditions, several parameters were measured in the field at each sampling site using a YODA (Yoing Ocean Data Acquisition) profiler (JFE Advantech Co. Ltd, Japan). Parameters included temperature, salinity, chlorophyll-a (Chl-a), turbidity, and dissolved oxygen (DO). Dissolved nutrients (NH_4^+, SiO_4^{4-}, PO_4^{3-}, and NO_x) were quantified spectrophotometrically (Shimadzu, UV-1650PC, Japan). The detection limit of each species is NH_4^+: 0.2 μM, SiO_4^{4-}: 0.1 μM PO_4^{3-}: 0.1 μM and NO_x: 0.2 μM. Specifically, the indolphenol, Cu-cd reduction, ascorbic acid, and molybdenum blue methods were employed for colorimetric quantification of dissolved inorganic ammonium, nitrogen oxide, phosphate, and silicate in the filtrate, respectively (Strickland and Parsons, 1972).

2.3. DNA sample preparation and Miseq sequencing

Genomic DNA was extracted from filter samples using the NucleoSpin Soil kit (MN, Germany), following the manufacturer's instructions. The quality and quantity of DNA extraction were assessed using 1 % agarose gel electrophoresis and a NanoDrop (Thermo Scientific, Canada). Polymerase chain reaction (PCR) amplification was carried out with the extracted DNA using specific primer sets targeting the V4 region of 16S ribosomal RNA (rRNA) genes for bacteria (515F and 806R) and the V8–V9 region of 18S rRNA genes for phytoplankton (V8F and 1510R), as detailed in Supplementary Table S1. PCR conditions for bacterial and phytoplankton amplification were similar, differing only in the annealing temperature (55 °C for bacteria and 62 °C for phytoplankton). The PCR reaction mixture consisted of 10 μL of 2X Prime Taq Premix (GeNet Bio, Korea), 0.5 μL of 10 μM forward and reverse primers, 1 μL of sample DNA, and 8 μL of distilled water, totaling 20 μL. The first PCR involved an initial denaturation at 95 °C for 3 min, followed by 30 cycles of denaturation at 95 °C for 30 s, annealing at either 55 °C or 62 °C for 30 s, and extension at 72 °C for 30 s, with a final elongation cycle at 72 °C for 5 min. Amplicons were confirmed by electrophoresis on a 1.5 % agarose gel and purified using the Expin™ Gel SV Kit (GeneAll, Korea). A second PCR for barcoding DNA was performed with 5 μl of 1st PCR purified amplicon, 0.5 μl (10 pM) of each Illumina index primer, 4 μl of PCR grade water, and 10 μl of Prime Taq Premix (Genetbio, Co., Ltd., Daejeon, South Korea), for a final volume of 20 μl. PCR amplification was conducted similarly for 8 cycles under the same conditions. DNA concentration was determined using NanoDrop (Thermo Scientific, Canada) to ensure accurate quantification, and equal amounts of DNA from phytoplankton and bacteria were pooled in one Eppendorf tube. The samples were sent for further Miseq sequencing at Macrogen (Seoul, Korea).

2.4. Statistical analysis

Sequencing reads obtained from Illuminia Miseq reactions were processed in the R environment (v4.1.2) to determine the composition of phytoplankton and bacterial communities. The Divisive Amplicon Denoising Algorithm 2 (DADA2) pipeline (v1.22.0) was utilized for quality filtering, dereplication, denoising, merging, and chimera sequence checking, ultimately clustering reads into amplicon sequence variants (ASV) (Callahan et al., 2016; RCore, 2016). Taxonomic identification was determined by comparison to the Silva v 132 reference databases (Pruesse et al., 2007). The richness (Chao1 index) and diversity (Shannon index) of phytoplankton and bacterial communities were assessed using the phyloseq package. Principal Coordinates Analysis (PCoA) based on Bray-Curtis distances were performed to visualize community composition differences among samples. To evaluate these differences, Analysis of Similarity (ANOSIM) using Bray-Curtis distance was conducted with the vegan package. Graphical representations were generated using ggplot2 (v3.4.2). Pearson correlation analysis was employed through the corrplot (v0.92) and Hmisc (v5.0-1) R packages. Data analysis utilized SigmaPlot software (version 12.5; Systat, San Jose, CA), with results presented as mean ± standard deviation. Statistical significance was determined using a two-tailed *t*-test with $p < 0.05$ considered indicative of a significant difference. A heat map using the abundances of the top 50 ASVs at the class level was generated using Microsoft Excel. Sequence data of both 16S rRNA and 18S rRNA genes obtained from this study were deposited in the ENA Short Read Archive under the accession number PRJNA1196622.

2.5. QPCR for bacteria and phytoplankton analysis

To assess the abundance of microbial and phytoplankton communities in YS samples, quantitative PCR (qPCR) analysis was performed using genomic DNA extracted from filter paper samples, diluted to a concentration of 10 ng/μL for use as qPCR template preparation. For bacterial analysis, the 515F-Y forward primer and 806R reverse primer targeting the V4 region of the 16S ribosomal RNA gene were used (Supplementary Table S1). The PCR reaction mixture was composed of 10 μL of SYBR-Premix Ex Taq II (Takara Bio, Japan), 0.4 μL of ROX, 1 μL each of 5 μM forward and reverse primers, 1 μL of sample DNA, and 6.6 μL of distilled water, totaling 20 μL. PCR conditions consisted of an initial denaturation at 95 °C for 5 min, followed by denaturation at 95 °C for 30 s, annealing at 52 °C for 30 s, and extension at 72 °C for 30 s, repeated over 30 cycles. The final melt curve stage comprised melting at 95 °C for 15 min, followed by annealing at 52 °C for 1 min and extension at 95 °C for 15 s. For phytoplankton analysis, the forward P23MISQF1 and reverse P23MISQR1 primers targeting the 23S rRNA gene were used with an altered annealing temperature of 55 °C.

To establish bacterial qPCR standards, the 16S rRNA gene of *Bacillus cereus* DNA was amplified with universal 27F and 1492R primers, and the resulting amplicons were purified using the Expin™ Gel SV Kit (GeneAll, Korea). Quantitative values were determined by calculating copies per 1 mL of seawater, which were then converted to a log scale. Only coefficients of determination (R^2) for standard curves ≥0.99 and qPCR efficiencies (E)≥80 % were accepted. Similarly, a qPCR standard for phytoplankton communities was generated by amplifying the 23S rRNA gene of *Chaetoceros muelleri* DNA using P23MISQF1 and P23MISQR1 primers, running a 1 % agarose gel, and purifying the amplified product using the Expin™ Gel SV Kit (GeneAll, Korea).

3. Results

3.1. Environmental parameters

Environmental parameters including temperature, salinity, chlorophyll *a* (Chl-a), turbidity, DO, nitrogen oxide (NO_x), ammonia, silicate, and phosphate concentrations, varied by site and season (Table 1). The average temperature ranged from 18.20 °C in May at TY to 24.47 °C in August at the same location. The highest average salinity was 32.38 psμ in May at TY, while other sites showed similar salinity levels between 31.05 psμ and 31.88 psμ, indicating no significant variance in temperature and salinity among the samples. Chl-a levels were generally consistent across the sampling sites, averaging from 0.84 to 1.07 μg/L, except for a notable peak of 45.56 μg/L in the August samples from YS. In August, Chl-a values in YS showed an increasing trend from site 1 to site 5, with concentrations reaching 58.42 μg/L and 79.33 μg/L at sites 4 and 5, respectively, indicating a *Cochlodinium polykrikoides* bloom. In September, the average Chl-a concentration across the five sites in YS was 1.02 ± 0.38 μg/L, showing a statistically significant difference compared to August levels (*t*-test, $p < 0.05$). In contrast, no significant changes in Chl-a levels were observed at TY between August and September. Turbidity varied significantly depending on sampling sites and months, with averages ranging from 4.0 to 104.42 FTU (*t*-test, $p < 0.05$). DO remained stable (89.92 %–101.36 %), whereas nutrients (NO_x, NH_4^+, SiO_4^{4-}, and PO_4^{3-}) declined in YS during August.

3.2. Bacteria and phytoplankton QPCR abundance

In YS, the average bacterial abundance in August samples was $(2.0 \pm 3.22) \times 10^5$ copies/mL, ranging from 5.78×10^3 to 8.35×10^5 copies/mL. By September, this average had significantly decreased to $5.68 \pm 2.4) \times 10^3$ copies/mL, ranging from 2.41×10^3 to 8.38×10^3 copies/mL, representing an approximate 35.2-fold decrease (Fig. 2A). Notably, sites 4 and 5, which had high Chl-a values in August, showed much higher bacterial abundances of 1.42×10^5 and 8.35×10^5 copies/mL, respectively. These abundances dropped to 8.38×10^3 and 7.73×10^3 copies/mL in September, indicating that bacterial levels were approximately 17 and 108 times higher in August at sites 4 and 5, respectively.

Phytoplankton abundance also changed between August and September in YS. Phytoplankton abundance dropped from $(1.0 \pm 0.7) \times$

Table 1
List of samples used in this study and sampling details including the coordinates of the sampling sites and environmental parameters observed at each location. TY and YS represent Tongyeong and Yeosu, respectively.

Sample	Date of Sampling Month/ Year	Location	Longitude	Latitude	Temperature (°C)	Salinity (psu)	Chl-a (μg/l)	Turbidity (FTU)	DO (%)	NOx (μM)	Ammonia (μM)	Silicate (μM)	Phosphate (μM)
TY5-1	May-2022	TY	34.78125	128.3801	17.89	33.46	1.64	43.75	102.29	0.20	0.13	0.05	0
TY5-2	May-2022	TY	34.78125	128.3881	18.04	28.34	0.64	1.61	96.09	0.11	0.06	0.07	0.01
TY5-3	May-2022	TY	34.76848	128.3841	18.04	33.42	0.82	0.73	101.09	0.08	0.02	0.07	0
TY5-4	May-2022	TY	34.75571	128.3801	18.52	33.25	0.38	97.43	97.41	0.12	0.02	0.07	0.00
TY5-5	May-2022	TY	34.75571	128.3881	18.51	33.44	0.72	0.46	98.18	0.12	0.06	0.07	0.01
Average					18.2 ± 0.29	32.38 ± 2.26	0.84 ± 0.83	28.8 ± 42.62	99.01 ± 2.59	0.13 ± 0.04	0.06 ± 0.04	0.07 ± 0.01	0 ± 0.01
TY8-1	Aug-2022	TY	34.77699	128.3774	24.49	32.66	0.69	0.51	104.48	0.05	0.01	0.07	0.01
TY8-2	Aug-2022	TY	34.77699	128.3881	24.61	32.69	0.57	0.95	100.17	0.06	0.01	0.08	0.01
TY8-3	Aug-2022	TY	34.76423	128.3814	24.44	32.64	0.75	0.88	98.95	0.05	0.02	0.06	0.01
TY8-4	Aug-2022	TY	34.7472	128.3774	24.38	29.58	0.54	0.06	95.63	0.05	0.02	0.06	0.01
TY8-5	Aug-2022	TY	34.7472	128.3881	24.42	27.70	2.80	77.46	103.83	0.05	0.01	0.07	0.01
Average					24.47 ± 0.09	31.05 ± 2.30	1.07 ± 0.97	15.97 ± 34.38	100.61 ± 3.64	0.05 ± 0.00	0.01 ± 0.01	0.07 ± 0.01	0.01 ± 0
TY9-1	Sep-2022	TY	34.77699	128.3774	23.59	31.65	1.64	0.39	96.91	0.16	0.02	0.04	0.00
TY9-2	Sep-2022	TY	34.77699	128.3881	22.10	32.62	1.68	18.26	103.87	0.08	0.02	0.04	0.00
TY9-3	Sep-2022	TY	34.76423	128.3814	23.58	31.59	1.60	0.53	97.94	0.04	0.02	0.04	0.00
TY9-4	Sep-2022	TY	34.7472	128.3774	23.57	31.61	1.61	0.39	99.63	0.04	0.02	0.04	0.00
TY9-5	Sep-2022	TY	34.7472	128.3881	23.52	31.59	1.61	0.43	99.07	0.04	0.02	0.05	0.00
Average					23.27 ± 0.65	31.81 ± 0.45	1.63 ± 0.03	4.00 ± 7.97	99.48 ± 2.67	0.07 ± 0.05	0.02 ± 0.00	0.04 ± 0.00	0 ± 0.00
YS8-1	Aug-2022	YS	34.35251	127.326	23.10	31.70	26.70	53.87	104.37	0.50	0.70	7.21	0.29
YS8-2	Aug-2022	YS	34.35074	127.3303	23.60	31.80	29.56	60.08	100.13	0.40	0.10	8.81	0.60
YS8-3	Aug-2022	YS	34.34487	127.3329	23.70	31.90	33.78	67.69	101.98	0.40	0.30	10.08	0.36
YS8-4	Aug-2022	YS	34.34455	127.333	24.10	31.70	58.42	137.04	100.20	0.70	0.20	9.88	0.43
YS8-5	Aug-2022	YS	34.34452	127.3339	24.00	32.30	79.33	203.41	100.15	0.70	0.20	10.08	0.53
Average					23.7 ± 0.39	31.88 ± 0.25	45.56 ± 22.67	104.42 ± 64.68	101.36 ± 1.85	0.54 ± 0.15	0.3 ± 0.23	9.21 ± 1.24	0.44 ± 0.13
YS9-1	Sep-2022	YS	34.35251	127.326	24.20	31.50	1.74	3.57	91.68	0.90	3.30	12.88	0.43
YS9-2	Sep-2022	YS	34.35074	127.3303	23.90	31.40	1.02	4.75	92.39	1.90	1.20	11.64	0.51
YS9-3	Sep-2022	YS	34.34487	127.3329	24.10	31.40	0.82	3.02	87.46	2.70	3.20	24.39	0.63
YS9-4	Sep-2022	YS	34.34455	127.333	24.30	31.40	0.65	3.94	87.89	1.30	1.90	19.50	0.49
YS9-5	Sep-2022	YS	34.34452	127.3339	24.30	31.50	0.89	6.18	90.16	0.80	1.80	14.79	0.38
Average					24.16 ± 0.17	31.44 ± 0.05	1.02 ± 0.42	4.29 ± 1.23	89.92 ± 2.20	1.52 ± 0.79	2.28 ± 0.93	16.64 ± 5.26	0.49 ± 0.09

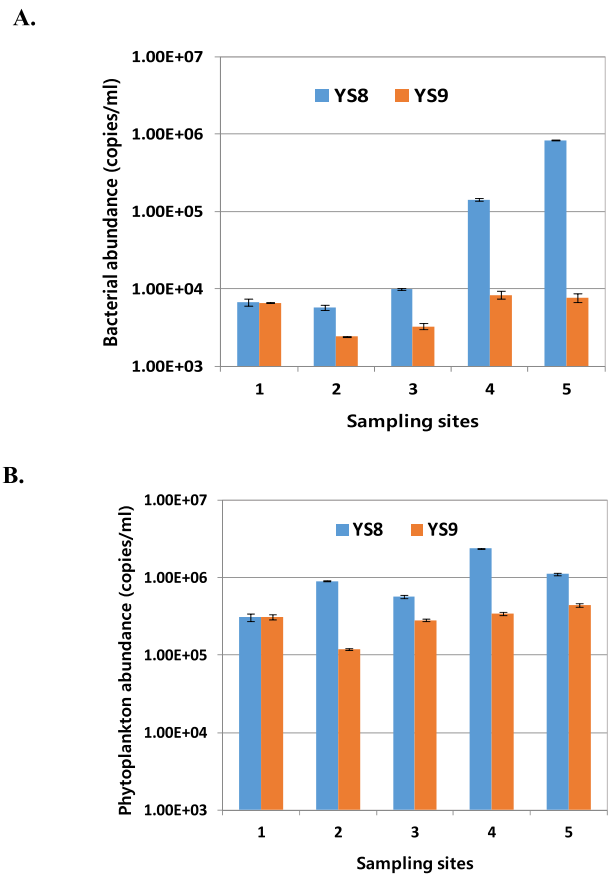

Fig. 2. QPCR amplification of bacterial (**A**) and phytoplankton (**B**) DNA from samples collected at various sites in YS during August (YS8) and September (YS9).

10^6 copies/mL (August) to $(3.0 \pm 1.0) \times 10^5$ copies/mL (September). Unlike the bacterial abundance, there were no significant differences in phytoplankton abundance at sites 4 and 5. However, overall phytoplankton levels in August were about 3.5 times higher on average compared to September (Fig. 2B).

3.3. Microbial taxonomic analysis

In our investigation of bacterial communities, we initially obtained a total of 1,708,722 16S rRNA gene reads. Following the removal of chimera sequences and low-quality reads, 1,311,432 high-quality reads remained, averaging 52,457 reads per sample as detailed in Supplementary Table S2. These high-quality reads were subsequently classified into 2053 ASVs for further taxonomic analysis. The distribution of major taxonomic groups at the phylum level is depicted in Fig. 3A. Proteobacteria (60.02 %) was the most dominant phylum, followed by Cyanobacteria (15.14 %), Bacteroidetes (13.76 %), Actinobacteria (3.76 %), Euryarchaeota (2.64 %), Verrucomicrobia (1.60 %), and Planctomycetes (1.11 %), etc.

In TY, during May, the bacterial community at the phylum level was dominated by Proteobacteria, which exhibited the highest abundance (89.90 %), followed by Cyanobacteria (4.96 %) and Bacteroidetes (3.35 %). However, by August, although Proteobacteria retained dominance, their proportion significantly decreased to 36.94 %, while the other bacterial groups, such as Bacteroidetes and Actinobacteria, increased to 28.47 % and 10.05 %, respectively. Subsequently, in September, overall proportions remained similar to August, except for a significant decline in Actinobacteria from 10.05 % to 1.38 %.

In YS, during August, there was a marked increase in the proportions of Proteobacteria to 80.22 % compared to August in TY. Also, Cyanobacteria and Bacteroidetes decreased to 10.76 % and 5.4 %, respectively. Furthermore, a comparison of the Proteobacteria dominant proportions among the August samples in YS revealed an increasing trend, especially in samples 4 and 5, which are located farthest from the coastline. In September in YS, while the proportions of Proteobacteria significantly decreased to 46.98 %, other groups such as Cyanobacteria and Bacteroidetes increased, which is a similar trend observed in TY during September. However, the proportions of archaea groups, such as Euryarchaeota and Thaumarchaeota, significantly increased to 12.68 %, indicating a noteworthy shift from their relatively minor presence in other samples. At the family level, Altermonadaceae and Pseudoaltromonadaceae dominated in May at TY, while Vibrionaceae were prevalent in August at YS (Fig. 3B). Heatmap analysis of the top 50 ASVs revealed variations in the microbial community across sampling months and locations (Fig. 4). The dominant bacterial phyla were Proteobacteria and Cyanobacteria. In TY, at the class level, Alphaproteobacteria increased in both August and September, while Gammaproteobacteria decreased compared to May. In contrast, during August in YS, Alphaproteobacteria decreased and Gammaproteobacteria increased, particularly in samples 4 and 5, revealing a similar trend observed in TY in May. However, the dominant Gammaproteobacteria ASVs differed between TY's May and YS's August data.

3.4. Eukaryotic taxonomic analysis

This study analyzed the eukaryotic community compositions in various samples. Initially, a total of 1,683,771 raw sequence reads were obtained (Supplementary Table S3). After quality control, we retained 934,382 high-quality reads, with an average of 37,375 reads per sample. These sequences were further classified into 1940 ASVs. The major taxonomic groups at the phylum level are detailed in Fig. 5A. The phylum Arthropoda exhibited the highest dominance at 42.73 %, followed by Dinoflagellata (27.08 %), Protalvelolata (10.79 %), Ochrophyta (8.01 %), Cnidaria (2.59 %), and Ciliophora (2.27 %), etc.

In TY, during May, the eukaryotic community was predominantly composed of Arthropoda (72.42 %), with Dinoflagellata (12.98 %) and Ocrophyta (7.00 %) as subdominant groups. By August, while Arthropoda remained dominant, its proportion decreased significantly to 46.65 %. In opposite, Dinoflagellata and Ciliophora increased to 30.09 % and 7.40 %, respectively. By September, the proportion of Arthropoda increased again to 64.48 %, accompanied by a diverse subdominant assemblage including Ochrophyta (12.80 %), Dinoflagellata (8.36 %), Protalveolata (4.44 %), and Cnidaria (3.90 %).

In YS, distinct eukaryotic communities were observed compared to TY. During August, Dinoflagellata dominated the community at the phylum level (78.37 %), followed by Arthropoda (8.96 %), Ochrophyta (8.63 %), and Cnidaria (1.24 %). Notably, Dinoflagellata showed an increasing trend, reaching over 90 % dominance in both samples 4 and 5, which is a similar trend observed in bacterial community analysis. By September, Protalveolata became the dominant group (44.04 %), followed by Arthropoda (21.16 %), Ochrophyta (7.75 %), and Cnidaria (6.37 %). However, the dominance Dinoflagellata observed in August significantly decreased to 5.59 % by September. At the genus level, *Cochlodinium* was predominant in August at YS (Fig. 5B). The heatmap analysis of the top 50 ASVs also demonstrated similar variations in the eukaryotic community across different sampling months and locations (Fig. 6). In TY, the dominant eukaryotic phylum was Arthropoda. At the class level, some ASVs belonging to Dinophyceae and Noctilucales showed an increasing trend in August, although these changes were not significant. In contrast, in YS during August, one ASV from the Dynophyceae class proliferated significantly but disappeared by September. Additionally, in YS, some ASVs from the Syndiniales class increased in September.

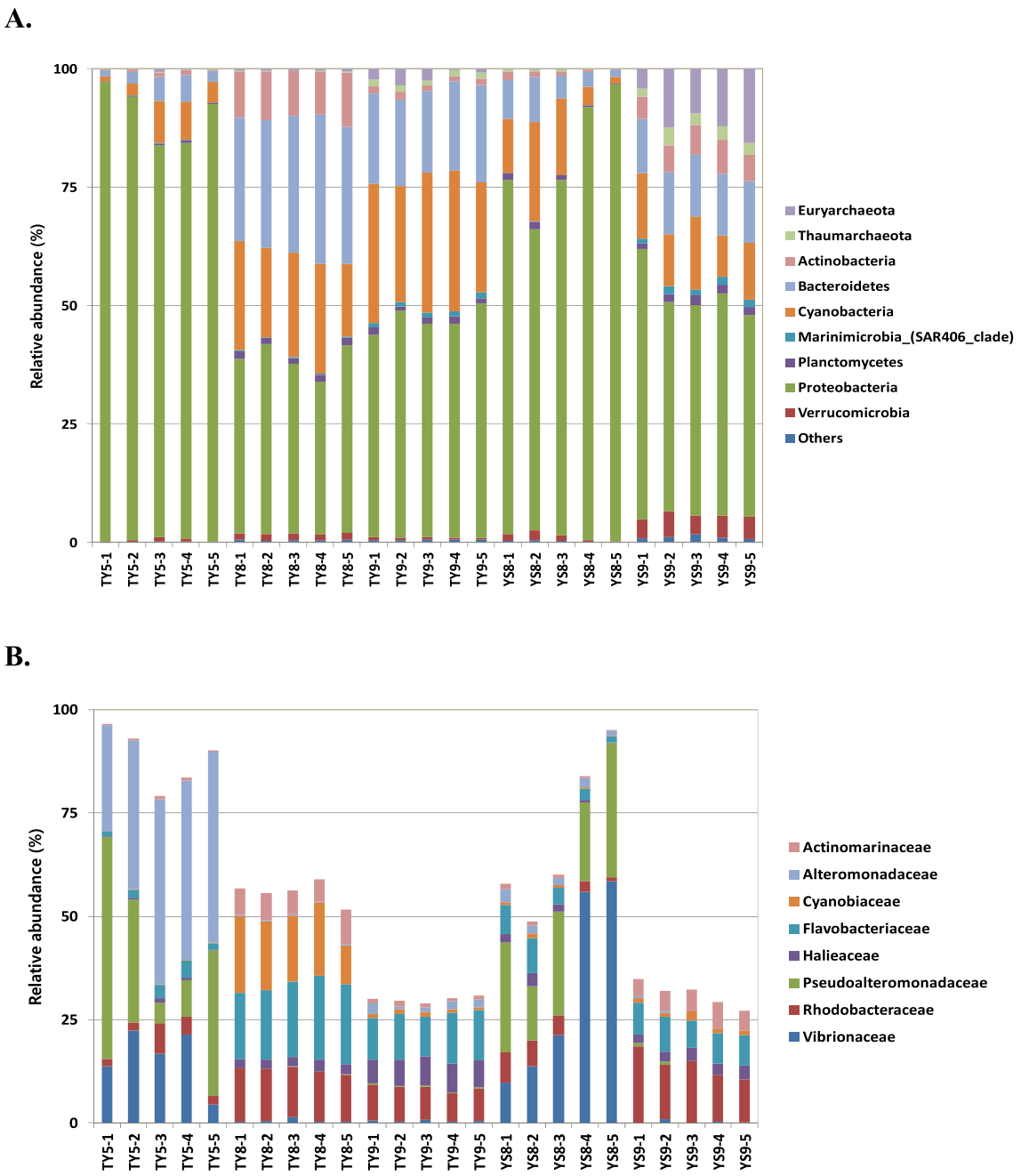

Fig. 3. The taxonomic distribution of the microbial community is shown at the phylum level (**A**) and family level (**B**), with bar heights indicating the relative proportions of each group. Only microbes with a relative abundance greater than 1 % are shown at the phylum level (**A**), while those exceeding 10 % are included at the family level (**B**).

3.5. Diversity and composition of bacterial and eukaryotic communities

The diversity of both bacterial and eukaryotic communities, measured using ASV number, Chao1, ACE, and Shannon indices, is summarized in Supplementary Tables S4 and S5. In TY, bacterial alpha diversity was lowest in May, compared to August and September, with no significant variations among sampling sites. In YS, bacterial diversity was similar between August and September, although it decreased from site 1 to site 5 in August, a trend not observed in TY. Eukaryotic diversity showed similar trends. TY showed the lowest diversity in May, with no significant differences among sites in August and September, whereas in YS, the lowest diversity was observed at sampling sites 4 and 5 in August. Bacterial Shannon diversity dropped significantly at YS bloom sites, reflecting reduced evenness.

PCoA analysis revealed differences in bacterial and eukaryotic communities based on sampling months and locations (Supplementary Fig. S1A and S2A). For bacterial communities, May samples from TY clustered in the upper left of the plot, while August and September samples were located in the opposite right. In YS, significant differences were observed between bacterial communities in August and September. For eukaryotic communities, samples from May, August, and September clustered relatively well in TY, while August and September samples in YS showed significant differences.

CAP analysis demonstrated the relationship between eukaryotic community structure and environmental variables (Supplementary Fig. S1B and S2B). In YS, both bacterial and eukaryotic communities in August were correlated with high levels of chlorophyll and turbidity. Pearson correlation analysis of the four most abundant genera of

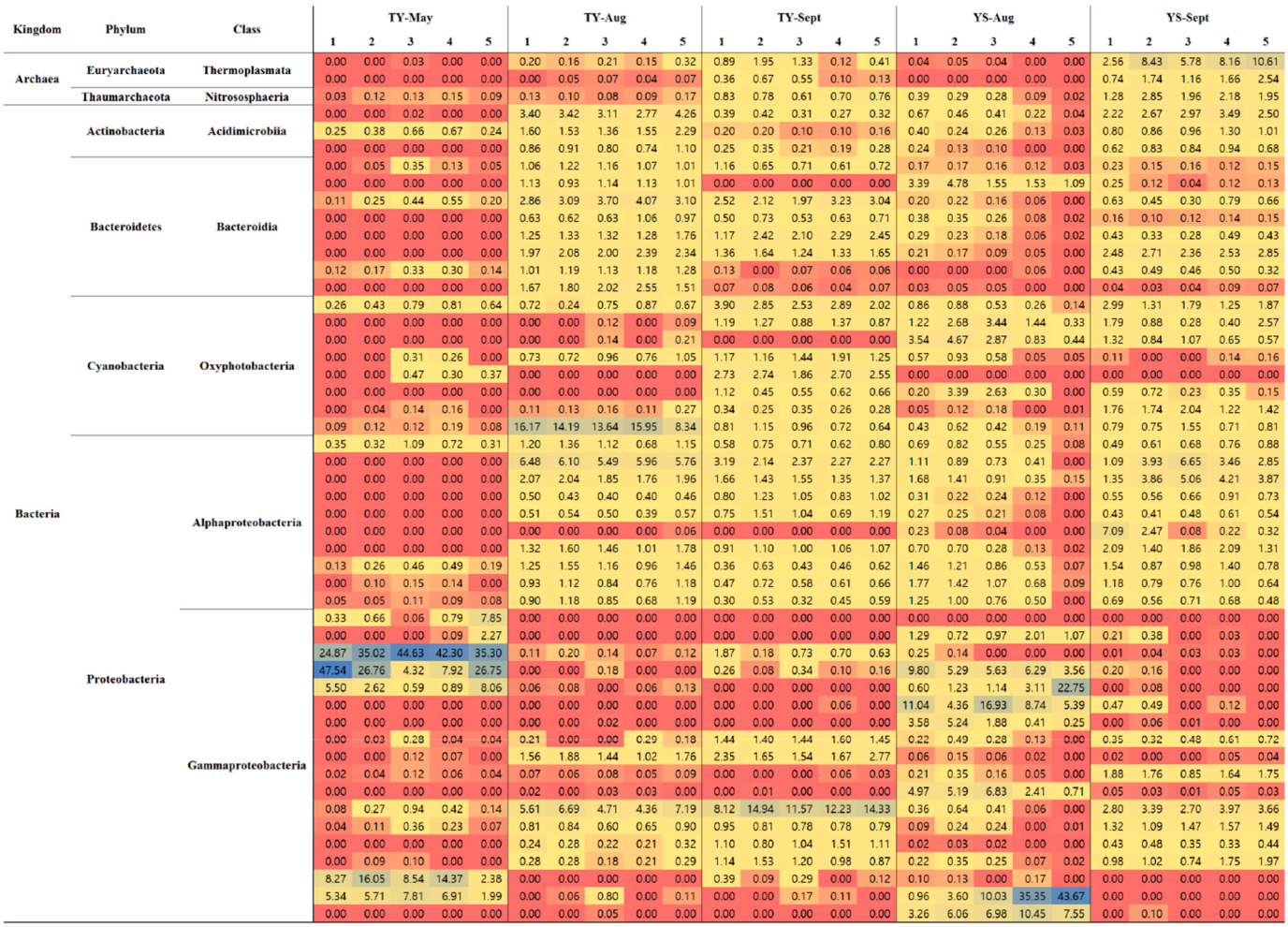

Fig. 4. A heatmap displaying the relative abundance of the top 50 abundant microbial ASVs in TY and YS samples is shown.

phytoplankton and the ten most abundant genera of bacteria in August in YS revealed a significant positive correlation between *Cochlodinium* and the bacteria *Vibrio* and *Pseudoalteromonas* ($p < 0.05$), with correlation coefficients of 0.763 and 0.931, respectively (Fig. 7).

4. Discussion

4.1. May of TY

Observations at TY in May provide strong evidence supporting our hypothesis that top-down control is a critical factor in shaping marine ecosystems, particularly through the interactions between zooplankton and phytoplankton. The moderate increase in Chl-a without algal blooms (18S rRNA data), together with high copepod abundances, suggests that zooplankton grazing suppressed phytoplankton biomass (Fig. 5 and Table 1). These results suggest that phytoplankton populations are regulated not primarily by nutrient availability (bottom-up factors), but by grazing pressures from zooplankton. This is further supported by the significant increase in copepod abundances, known herbivores of phytoplankton (Huys and Boxshall, 1991). Despite favorable growth conditions for phytoplankton, intense zooplankton grazing suppressed phytoplankton biomass, demonstrating the complexity of these ecological interactions. While most studies emphasize nutrient-driven (bottom-up) regulation, our data support top-down control as equally critical (Odate and Imai, 2003; Sommer, 2000). For instance, research in the northeastern continental shelf of the Gulf of Cadiz has similarly emphasized the top-down control as a key regulatory force (Rodríguez-Gálvez et al., 2023). Although direct evidence of zooplankton-driven top-down effects on phytoplankton dynamics in natural field conditions has been limited (Odate and Imai, 2003; Stenseth et al., 2006), this may be due to methodological problems or the sporadic nature of top-down influences, which can occur only under specific ecological conditions. Nevertheless, our study provides important evidence for the role of zooplankton grazing in shaping marine ecosystem structure.

Our analysis of microbial community shifts, using 16S rRNA sequencing combined with PCoA and CAP analyses, further reveals the complexity of marine ecosystem interactions. Although algal biomass accumulation (i.e., algal blooming) was absent due to top-down control, *Pseudomonas* and *Vibrio* taxa also dominant during YS August blooms, suggesting shared organic matter niches (Figs. 3 and 5). Under top-down control, primary productivity remains high despite low to moderate phytoplankton biomass, and organic detritus production increases (Table 2). This increased detritus production likely supports microbial groups that are similar to those found during algal blooms.

While both phytoplankton and zooplankton contribute organic matter that supports bacterial growth, bacteria can also influence phytoplankton composition (Azam et al., 1983; Buchan et al., 2014; Costas-Selas et al., 2022). However, our findings indicate that the bacterial genera such as *Altermonas* and *Pseudoaltermonas*, dominated without a corresponding shift in phytoplankton composition, suggesting that limited bacterial influence on primary producers during this period. This observation highlights the idea that zooplankton grazing was the primary driver of phytoplankton biomass regulation at this time.

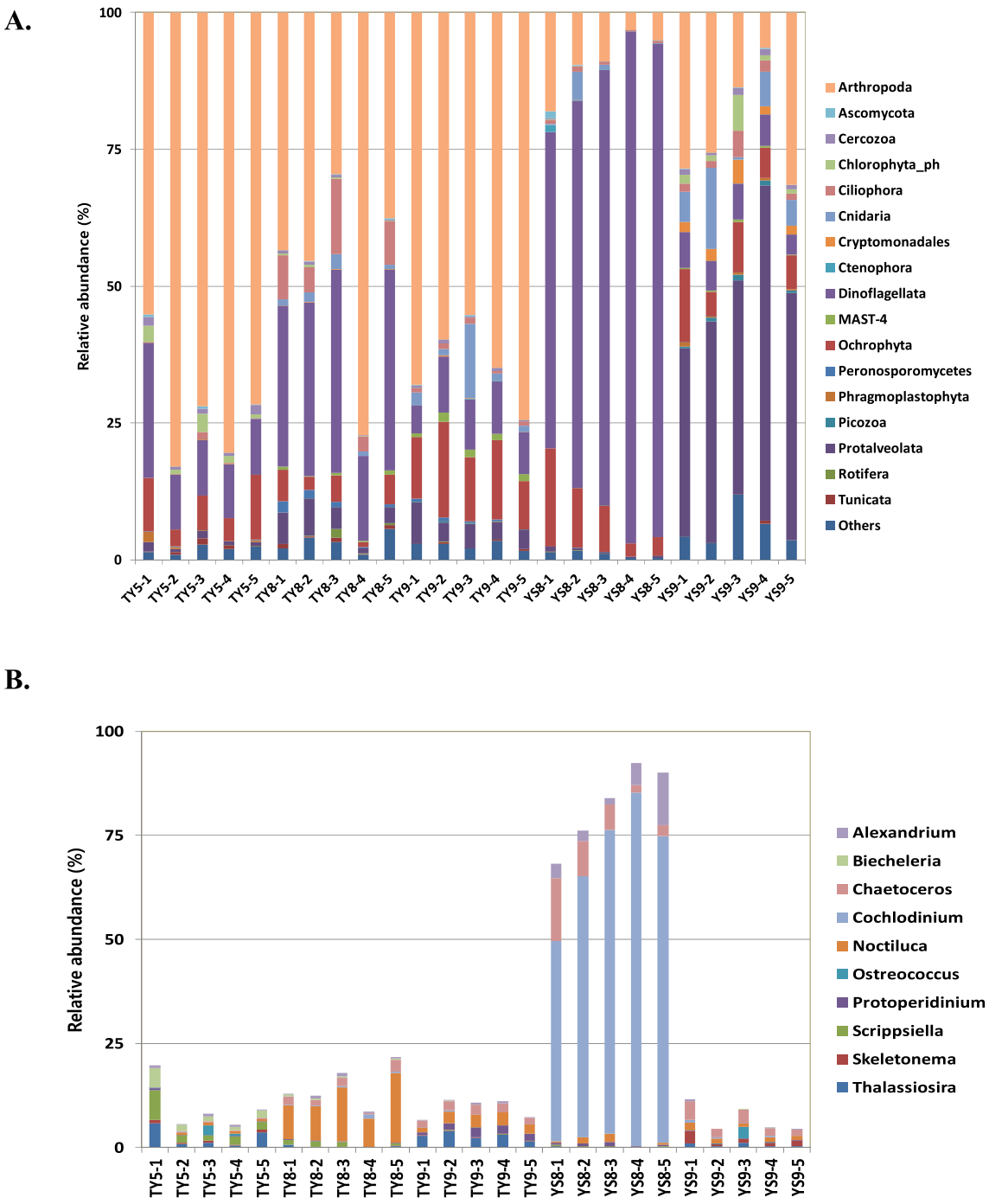

Fig. 5. The taxonomic distribution of the eukaryotic community is depicted at the phylum level (**A**) and genus level (**B**), with bar heights indicating the relative proportions of each group. Only phytoplankton groups with a relative abundance greater than 1 % are shown at the phylum level (**A**), while those exceeding 10 % are included at the genus level (**B**).

Overall, our findings from May reveal the complex and interconnected dynamics within marine ecosystems.

4.2. August and September of TY

In August and September, the environmental conditions at TY shifted significantly, revealing the transition to late summer and early fall in South Korea's coastal waters. The observed decrease in nutrient concentrations and Chl-a levels indicated a period of relatively low nutrient availability, typical of this time of year (Table 2). Our 18S rRNA analysis revealed an increase in the relative abundance of certain phytoplankton groups, such as *Dinoflagellata* and *Ochrophyta*, suggesting that these species are better adapted to nutrient-limited conditions, likely due to their unique functional traits (Tilman et al., 1982; Interlandi and Kilham, 2001). Additionally, the dominance of *Cyanobacteria*, which can utilize organic nutrients and enhance productivity through nitrogen fixation, suggests a role in sustaining productivity under nutrient-limited conditions (Issa et al., 2014; Zubkov et al., 2003). Declining zooplankton pressure (evidenced by shifting phytoplankton) weakened top-down control. As zooplankton grazing pressure decreased, microbial community structures were less impacted, resulting in a more diverse microbial community. Our 16S rRNA analysis,

Kingdom	Phylum	Class	TY-May					TY-Aug					TY-Sept					YS-Aug					YS-Sept				
			1	2	3	4	5	1	2	3	4	5	1	2	3	4	5	1	2	3	4	5	1	2	3	4	5
Eukaryota	Arthropoda	Maxillopoda	0.53	75.63	69.39	78.29	18.81	29.98	40.63	16.27	72.79	21.45	55.49	40.21	43.46	47.48	66.27	1.52	0.05	3.07	0.64	0.22	20.46	24.97	2.91	3.02	29.59
			48.64	0.00	0.05	0.00	0.00	0.09	0.02	0.53	0.00	4.78	0.03	0.00	0.00	0.00	0.00	7.10	0.20	0.00	0.00	0.01	0.00	0.00	0.00	0.03	0.00
			0.00	0.01	0.00	0.00	0.00	10.41	3.61	10.22	0.70	6.39	0.00	0.08	0.00	0.19	0.00	6.55	7.88	5.55	2.44	2.41	0.00	0.00	0.20	0.06	0.17
			0.00	0.00	0.00	0.00	39.26	0.00	0.04	0.00	0.00	0.00	0.00	7.40	4.29	6.57	0.03	0.21	0.00	0.00	0.00	0.00	0.00	0.00	0.00	0.10	0.00
			0.07	0.00	0.00	0.00	0.00	1.69	0.18	0.28	0.06	0.39	3.76	10.03	2.94	5.30	3.85	0.26	0.00	0.00	0.00	0.00	7.95	0.69	10.56	2.39	1.72
			5.77	6.15	1.42	1.62	12.37	0.00	0.24	0.94	1.81	0.06	0.24	0.00	0.11	0.10	0.14	0.05	1.01	0.00	0.00	0.00	0.00	0.00	0.00	0.04	0.00
			0.00	0.27	0.35	0.30	0.00	0.51	0.57	0.50	0.59	0.00	0.45	0.00	0.00	0.00	0.32	0.00	0.00	0.00	0.00	0.00	0.00	0.00	0.00	0.00	0.00
			0.00	0.00	0.00	0.00	0.00	0.00	0.00	0.00	0.00	0.00	3.63	0.00	0.55	0.00	0.00	0.00	0.00	0.00	0.00	0.00	0.00	0.00	0.00	0.00	0.00
			0.00	0.00	0.00	0.00	0.00	0.00	0.00	0.00	0.00	0.00	1.22	0.00	0.69	1.89	0.48	0.00	0.00	0.00	0.00	0.00	0.00	0.00	0.00	0.00	0.00
	Ascomycota	Eurotiomycetes	0.11	0.08	0.51	0.03	0.00	0.06	0.20	0.05	0.00	0.21	0.06	0.03	0.28	0.04	0.04	1.23	0.11	0.00	0.00	0.05	0.14	0.02	0.03	0.20	0.00
	Chlorophyta_ph	Mamiellophyceae	0.00	0.00	0.00	0.00	0.00	0.00	0.00	0.00	0.00	0.00	0.05	0.00	0.04	0.00	0.00	0.00	0.00	0.00	0.00	0.00	0.83	0.46	1.47	0.51	0.48
	Ciliophora	Intramacronucleata	0.00	0.00	0.00	0.00	0.00	3.97	0.93	6.65	0.18	1.74	0.00	0.00	0.00	0.00	0.00	0.02	0.00	0.00	0.00	0.00	0.00	0.00	0.00	0.00	0.00
	Cnidaria	Hydrozoa	0.00	0.00	0.00	0.00	0.00	0.00	0.00	0.00	0.00	0.09	2.03	0.97	1.06	0.54	0.83	0.01	0.09	0.04	0.00	0.00	5.54	14.85	0.35	6.15	4.67
			0.00	0.00	0.00	0.00	0.00	0.00	1.53	2.23	0.73	0.57	0.38	0.09	1.24	0.47	0.16	0.16	4.95	0.70	0.03	0.11	0.00	0.00	0.00	0.00	0.01
			0.00	0.00	0.00	0.00	0.00	0.93	0.02	0.00	0.06	0.14	0.00	0.05	11.23	0.23	0.09	0.02	0.00	0.00	0.00	0.00	0.03	0.00	0.02	0.00	0.00
	Cryptomonadales	Cryptomonadales_cl	0.00	0.00	0.06	0.03	0.00	0.05	0.08	0.04	0.00	0.08	0.04	0.12	0.10	0.03	0.06	0.00	0.01	0.02	0.00	0.00	0.84	1.15	1.73	0.74	0.85
	Dinoflagellata	Dinophyceae	0.14	0.12	0.00	0.00	0.00	0.23	0.24	0.33	0.84	0.42	0.12	0.21	0.06	0.03	0.07	46.94	60.68	70.96	83.18	71.93	0.59	0.35	0.07	0.26	0.01
			5.63	2.85	0.74	2.27	1.62	5.06	12.66	6.23	2.46	2.61	0.68	0.63	0.39	0.44	0.35	0.67	0.27	0.15	0.27	0.21	0.18	0.24	0.28	0.23	0.00
			0.00	0.00	0.00	0.00	0.00	0.08	0.42	0.46	0.06	0.45	0.04	0.00	0.00	0.00	0.07	2.39	2.26	1.13	4.73	11.46	0.00	0.00	0.00	0.12	0.00
			6.10	1.48	0.85	1.45	1.55	0.00	0.00	0.00	0.00	0.00	0.00	0.00	0.00	0.00	0.00	0.00	0.00	0.00	0.00	0.00	0.00	0.00	0.00	0.00	0.00
			2.46	0.92	0.94	0.73	1.25	0.42	0.37	0.47	0.00	0.31	0.00	0.11	0.00	0.00	0.00	0.03	0.00	0.00	0.00	0.00	0.00	0.00	0.00	0.04	0.00
			2.00	0.96	1.54	0.88	1.65	0.00	0.00	0.00	0.00	0.00	0.00	0.00	0.00	0.00	0.00	0.00	0.00	0.00	0.00	0.00	0.00	0.00	0.00	0.00	0.00
			0.00	0.00	0.00	0.00	0.00	0.15	0.12	0.26	0.07	0.17	0.63	1.26	1.99	1.75	1.40	0.00	0.00	0.00	0.00	0.00	0.00	0.00	0.00	0.00	0.00
			0.00	0.25	0.05	0.18	0.12	0.00	0.00	0.00	0.00	0.00	0.00	0.00	0.00	0.00	0.00	0.04	0.11	0.03	0.18	0.28	0.40	0.53	0.48	0.91	0.85
			0.00	0.00	0.00	0.00	0.00	0.90	0.43	1.21	0.19	1.04	0.04	0.07	0.04	0.08	0.00	0.16	0.08	0.02	0.03	0.13	0.19	0.03	0.04	0.00	0.05
			0.00	0.00	0.00	0.00	0.00	1.48	0.25	0.48	0.26	0.52	0.31	0.26	0.18	0.16	0.30	0.00	0.05	0.05	0.00	0.00	0.00	0.00	0.00	0.06	0.00
			1.18	0.23	0.42	0.23	0.50	0.10	0.00	0.15	0.06	0.21	0.00	0.00	0.05	0.00	0.00	0.08	0.00	0.03	0.00	0.06	0.09	0.06	0.10	0.05	0.00
			0.00	0.00	0.00	0.00	0.00	1.01	1.13	1.07	0.00	0.53	0.00	0.00	0.00	0.14	0.00	0.12	0.00	0.05	0.00	0.00	0.00	0.00	0.00	0.00	0.00
			1.94	0.51	0.18	0.21	0.48	0.00	0.00	0.00	0.00	0.00	0.00	0.00	0.00	0.00	0.00	0.00	0.00	0.00	0.00	0.00	0.00	0.00	0.00	0.00	0.00
		Noctilucales	0.00	0.53	0.57	0.54	0.51	4.60	5.80	8.69	4.46	10.39	0.89	1.88	2.00	2.13	1.77	0.00	0.68	1.00	0.00	0.36	0.43	0.87	0.54	0.58	0.47
			0.00	0.07	0.12	0.07	0.00	0.70	1.24	1.49	0.74	3.64	0.11	0.28	0.36	0.30	0.30	0.00	0.11	0.20	0.00	0.00	0.06	0.11	0.06	0.10	0.00
			0.00	0.00	0.00	0.00	0.00	0.76	1.02	1.41	0.83	1.42	0.00	0.24	0.40	0.32	0.33	0.00	0.11	0.17	0.00	0.00	0.00	0.00	0.00	0.00	0.00
			0.00	0.00	0.00	0.00	0.00	0.00	0.00	0.00	0.00	0.00	0.00	0.00	0.00	0.00	0.00	0.41	0.59	0.62	0.13	0.21	1.43	0.20	0.24	0.51	0.46
			0.00	0.00	0.00	0.00	0.00	2.09	0.20	1.10	0.53	1.17	0.00	0.00	0.00	0.00	0.00	0.00	0.00	0.00	0.00	0.00	0.00	0.00	0.00	0.00	0.00
	NA	NA	0.00	0.00	0.00	0.00	0.00	0.12	1.72	0.04	0.02	0.59	0.00	0.16	0.00	0.09	0.14	0.02	0.02	0.00	0.00	0.00	0.12	0.24	0.14	0.18	0.09
	Ochrophyta	Diatomea	0.04	0.02	0.07	0.06	0.11	0.15	0.27	0.11	0.04	0.18	0.12	0.11	0.08	0.12	0.05	15.06	8.44	6.10	1.75	2.65	4.34	1.90	3.32	1.84	1.45
			0.29	0.11	0.12	0.17	0.40	0.54	0.17	0.30	0.09	0.22	0.52	0.95	0.56	0.57	0.43	0.50	0.25	0.14	0.06	0.09	0.86	0.29	0.35	0.59	0.66
			0.00	0.00	0.04	0.00	0.00	0.00	0.00	0.00	0.00	0.04	0.22	0.34	0.18	0.21	0.16	0.30	0.34	0.59	0.29	0.23	1.13	0.24	0.14	0.46	1.08
			0.08	0.00	0.05	0.00	0.03	0.00	0.00	0.00	0.00	0.08	0.11	0.15	0.08	0.10	0.04	0.09	0.04	0.06	0.00	0.00	2.41	0.27	0.79	0.64	1.23
			2.55	0.38	0.61	0.33	1.49	0.00	0.00	0.00	0.00	0.00	0.00	0.00	0.00	0.00	0.00	0.00	0.00	0.00	0.00	0.00	0.00	0.00	0.00	0.00	0.00
			0.10	0.03	0.08	0.05	0.17	0.50	0.08	0.23	0.00	0.23	0.39	0.62	0.37	0.52	0.44	0.46	0.30	0.22	0.04	0.10	0.00	0.00	0.00	0.00	0.00
			0.00	0.00	0.00	0.00	0.00	0.00	0.00	0.00	0.00	0.00	1.05	1.52	0.64	1.02	0.47	0.00	0.00	0.00	0.00	0.00	0.18	0.00	0.34	0.00	0.00
			0.00	0.00	0.00	0.00	0.00	0.13	0.09	0.17	0.00	0.15	0.65	0.98	0.73	1.22	0.74	0.00	0.00	0.00	0.00	0.00	0.00	0.00	0.00	0.00	0.00
			1.56	0.16	0.28	0.12	0.83	0.00	0.00	0.00	0.00	0.00	0.00	0.00	0.00	0.00	0.00	0.14	0.05	0.07	0.03	0.04	0.18	0.04	0.11	0.08	0.11
	Peronosporomycetes	Peronosporomycetes_cl	0.00	0.00	0.00	0.00	0.00	1.07	1.44	0.85	0.22	0.19	0.00	0.00	0.00	0.00	0.00	0.01	0.01	0.00	0.00	0.02	0.00	0.00	0.00	0.00	0.00
	Protalveolata	Syndiniales	0.00	0.00	0.00	0.00	0.00	0.03	0.08	0.04	0.00	0.13	0.08	0.21	0.11	0.13	0.12	0.03	0.01	0.01	0.01	0.02	10.25	18.15	18.51	29.00	22.95
			0.00	0.00	0.00	0.00	0.00	0.00	0.08	0.00	0.00	0.15	6.55	1.42	2.78	1.95	2.41	0.12	0.00	0.00	0.00	0.00	10.51	10.01	5.71	8.42	6.79
			0.54	0.25	0.30	0.17	0.37	2.03	2.43	1.56	0.38	1.13	0.00	0.00	0.07	0.05	0.00	0.19	0.00	0.00	0.00	0.00	8.32	6.60	6.15	16.01	9.78
			0.03	0.03	0.28	0.11	0.00	0.04	0.05	0.05	0.00	0.07	0.00	0.03	0.00	0.05	0.00	0.00	0.00	0.00	0.00	0.00	2.13	1.63	2.68	3.13	1.98
			0.00	0.00	0.00	0.00	0.00	2.62	2.90	1.61	0.54	0.97	0.00	0.00	0.00	0.00	0.00	0.33	0.16	0.15	0.17	0.19	0.00	0.00	0.00	0.00	0.00

Fig. 6. A heatmap displaying the relative abundance of the top 50 abundant eukaryotic ASVs in TY and YS samples is shown.

along with PCoA and CAP data, revealed similar microbial communities during these months, with this pattern extending into September at YS (Supplementary Fig. S1). This suggests that the shifts observed at TY are not isolated but reflect broader regional influences. Interestingly, the stability of the microbial community structure, even over a distance of 120 km between TY and YS, indicates that the dynamics observed in late summer and early fall in the TY area are more representative of the southern coastal waters of South Korea, where the influence of higher trophic levels, such as zooplankton, is relatively weak.

4.3. August of YS

In August, during the harmful algal bloom (HAB) of *Cochlodinium* at YS, we observed strong evidence of the complex, multi-layered interactions between phytoplankton, zooplankton, and associated microbial communities. Elevated levels of Chl-a, DO, and turbidity reflected the intense photosynthetic activity typical of a severe bloom (Table 2). The dominance of *Cochlodinium*, confirmed through 18S rRNA sequencing, aligned with these high activity levels (Fig. 5). Notably, oversaturation of surface DO levels, which is uncommon due to atmospheric exchange, suggested active photosynthesis, consistent with the abundance of *Cochlodinium* (Table 1). The significant nutrient depletion during the bloom, evidenced by low nitrate and ammonium levels, showed how rapidly *Cochlodinium* utilized available nutrients for growth. Interestingly, we observed a low herbivorous copepod abundance during this period, indicating potential disruption in trophic

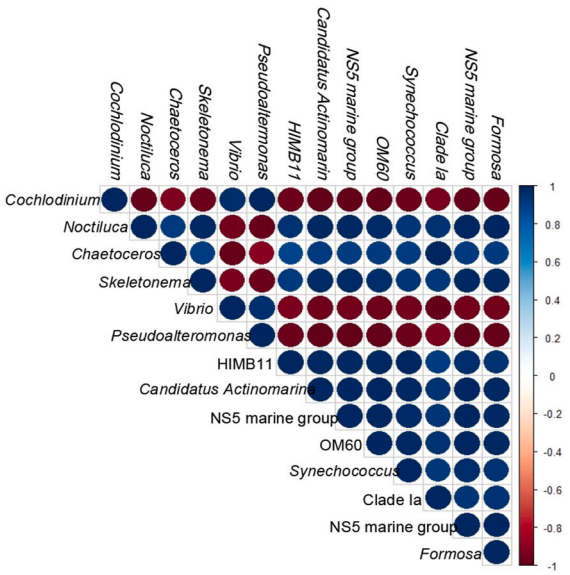

Fig. 7. Pearson correlation analysis of the most abundant plankton and bacteria genera reveals a significant positive correlation between *Cochlodinium* and the bacteria *Vibrio* and *Pseudoalteromonas* in August samples from YS. The genera *Cochlodinium*, *Noctiluca*, *Chaetoceros*, and *Skeletonema* are classified as planktonic microorganisms, whereas the remaining groups are classified under bacteria genera.

interactions, possibly due to extracellular polymeric substances (EPS) released by *Cochlodinium* (Fig. 5). These EPS compounds may interfere with zooplankton grazing, further reducing grazing pressure on the phytoplankton (Liu and Buskey, 2000).

The spatial gradient across sampling sites highlighted the role of location in influencing community structures. *Cochlodinium* was most dominant at offshore sites (4 and 5), while coastal sites (1, 2, and 3) showed lower levels, suggesting that factors other than nutrient availability, such as water dynamics and circulation patterns, may influence its distribution (Mitrovic et al., 2007; Sin and Lee, 2020). Offshore sites may provide physical conditions that favor *Cochlodinium* growth, while coastal sites, with more variable conditions, may support a more diverse phytoplankton community. In contrast, diatom abundance was higher at near-shore sites, despite lower silicate levels, suggesting that diatoms may actively deplete silicate. However, factors like light conditions or microbial interactions could also contribute to this pattern (Chen et al., 2009; Kuhlisch et al., 2024). Interestingly, lower diatom abundance at offshore sites, despite higher silicate levels, suggests that competition with *Cochlodinium*, possibly due to shading effects, may limit diatom growth (Fig. 6 and Table 1). This indicates that community structure is shaped by complex interactions, not just nutrient availability. The decline in diatom abundance from coastal to offshore sites corresponded with a decrease in copepod abundance, raising the idea that diatoms could be primary prey for copepods (Petrucciani et al., 2022). It would be an interesting study to explore whether lower copepod populations at offshore sites result from reduced food availability (diatoms), or other factors such as distinct physical conditions, or the influence of *Cochlodinium* EPS.

Primary organic matter sources play a crucial role in shaping microbial community structures (Kujawinski et al., 2016). While both May at TY and August at YS show high primary productivity, the types and quality of primary organic matter differ significantly between these systems. A key feature in August at YS was the accumulation of EPS produced by *Cochlodinium*. These EPS compounds may benefit the algae by aiding nutrient acquisition or providing protection from predators, but they can also have negative consequences for marine life, such as impairing fish respiration and causing local ecological imbalances (Richlen et al., 2010). The potential for EPS to act as a primary organic matter source for bacterial growth could influence microbial community composition. Our study found strong correlations between *Cochlodinium* and bacterial species, such as *Pseudomonas* and *Vibrio*, which thrive on the organic material excreted by algae. Similar bacterial groups were prevalent in both May at TY and August at YS, suggesting that these species are well-adapted to high organic matter availability. However, the correlations observed at TY in May were less specific, indicating a broader diversity of microbial interactions. In the TY system, where EPS dynamics were less pronounced, the microbial community likely relied more on other organic inputs, such as diverse phytoplankton-derived organic matter. This suggests that the type and quantity of primary organic matter, whether particulate or dissolved, significantly shape microbial communities.

This dynamic also reveals the importance of symbiotic relationships

Table 2
Overview of environmental and ecological characteristics and responses of major groups (zooplankton, phytoplankton and microbes) across TY and YS during the sampling months of May, August, and September. We hypothesize that the dominant types of organic matter-POM (Particulate organic matter), DOM (dissolved organic matter), OM (organic matter) and EPS (extracellular polymeric substances)-play significant roles in the ecological dynamics of these systems.

Parameters			May (TY5)	Aug (TY8)	Sept (TY9)	Aug (YS8) (* near land)	Sept (YS9)
Environmental Characteristics	Salinity		High	Medium (variable)	Medium	Medium	Medium
	Chlorophyll *a* (Chl-a)		Medium	Low	Medium	Very High	Medium
	Nitrate & Nitrite		Medium	Low	Low	Medium	High
	Ammonium		Medium	Low	Low	Medium	High
	Silicate		Low	Low	Low	High (*Medium)	High
	DO		Saturated	Saturated	Undersaturated	Oversaturated	Undersaturated
Group Relative Abundances	Zooplankton	Maxillopoda (Copepoda)	Very High	High (variable)	High	Low (*Medium)	Medium
	Phytoplankton	Dinoflagellate	Low	Low	Low	Very High	Low
		Diatom	High	Medium (variable)	Medium	Low (*Medium)	Low
		Syndiniales	Low	Low	Medium	Low	High
	Major Microbes		Vibrio Psudoalteromonadaceae Alteromonacacea	Cyanobacteria Rhodobacteraceae Flavobacteriacae	Rhodobacteraceae Flavobacteriacae Halieaceae	Vibrio Psudoalteromonadaceae Flavobacteriacae	Rhodobacteraceae Flavobacteriacae Actinomarinaceae
System Characteristics	Top-down control		Yes	No	No	Yes	Yes
	Nutrient Availability		Nutrient-rich	Nutrient-limited	Nutrient-limited	Nutrient-rich	Nutrient-rich
	Organic Matter Availability		High POM and DOM	Low OM	Low OM	High EPS	High Refractory DOM
	Microbial Diversity		Low	High	High	Low (High*)	High
	Blooming		No	No	No	Harmful Algal Bloom (HAB)	No

between algae and microbes. Algal species and microbes often show in a range of symbiotic interactions, including mutualism, commensalism, and parasitism, with mutualism being the most commonly observed type (Ramanan et al., 2016). A well-known example of mutualism involves marine algae like *Emiliania huxleyi* and heterotrophic bacteria like *Roseobacter*, where the algae benefit from essential micronutrients provided by the bacteria, which thrive in the nutrient-rich environment created by the algae (Ramanan et al., 2016; Geng and Belas, 2010). *Cochlodinium* and *Vibrio* may engage in mutualism, with bacteria supplying B-vitamins and algae providing organic substrates (Agarwal et al., 2019; Koch et al., 2012). Additionally, bacteria like *Vibrio* and *Pseudoalteromonas* are capable of hydrolyzing complex organic molecules such as glycosides, polysaccharides, and chitin, through enzymes like glycoside hydrolases and β-*N*-acetylhexosaminidase (Li et al., 2022; Miyoshi, 2013). These enzymatic activities enable bacteria to break down organic compounds into more accessible nutrients, potentially further influencing microbial community and nutrient cycling in marine ecosystems.

4.4. September of YS

In September, the observed decline in Chl-a indicated the end of the algal bloom peak, but it also triggers several broader ecological consequences. As Chl-a decreased, primary productivity declined, potentially altering energy flow through system. A key observation from heatmap analysis was the dominance of *Syndiniales*, a group of dinoflagellates that parasitize *Cochlodinium*, suggesting that complex predator-prey dynamics play a crucial role in regulating algal populations (Anderson and Harvey, 2020; Park et al., 2019). These interactions may act as a natural control mechanism, preventing *Cochlodinium* overabundance and moderating the impact of HABs. Following the bloom's collapse, undersaturated DO levels occurred, a direct consequence of organic matter decomposition (Table 1). This process can lead to hypoxic conditions, which pose significant threats to marine life, particularly benthic organisms (Levin et al., 2009; Zhang et al., 2015). Decomposition typically occurs at the sediment-water interface, where organic matter breakdown consumes oxygen and releases nutrients, such as ammonium and phosphate, back into the water column (Clavero et al., 2000). While decomposition in surface waters may be less intense than in bottom waters, elevated levels of ammonium, phosphate, and nitrate observed in this study indicate that nutrient cycling remained active throughout this period. Nitrifying bacteria (*Nitrosomonas*) likely drove ammonium to nitrate conversion, sustaining post-bloom productivity (Van Kessel et al., 2015). The increase in nitrifying bacteria, identified through 16S rRNA sequencing, supports the importance of microbial processes in maintaining nutrient dynamics during the post-bloom phase. Even in the absence of external nitrogen inputs, internal cycling of nutrients appears critical for sustaining ecosystem functioning and supporting primary production. Additionally, the observed increase in microbial diversity, along with similarities in microbial community composition between September at YS and TY, suggests that microbial communities in these systems are resilient to seasonal shifts and disturbances, including HABs. The seasonal succession of microbial communities indicates that while algal blooms can cause temporary disruptions, the system is capable of recovery and stabilization over time. Overall, these findings show the complex interplay between algal blooms, microbial dynamics, and nutrient cycling in coastal ecosystems. They highlight the importance of understanding the intricate relationships among primary producers, decomposers, and nutrient cycling processes in sustaining ecosystem stability.

5. Conclusions

Our study reveals how top-down (zooplankton grazing) and bottom-up (nutrient-driven) forces interact to shape marine ecosystems (Table 2). Shifts in phytoplankton (*Cochlodinium* to *Syndiniales*), microbial taxa (*Vibrio* dominance), and nutrient fluxes underscore the adaptability of the ecosystem. Microbial communities exhibited resilience, driving nutrient recycling and maintaining stability even during HABs and seasonal shifts. A comprehensive analysis of interactions among three trophic levels—bacteria, phytoplankton, and zooplankton—under both HAB and non-HAB conditions reveals critical ecosystem dynamics. High primary productivity can result in either bloom or non-bloom conditions, largely depending on zooplankton top-down control. However, bacterial responses appear to be similar in both scenarios, primarily driven by the availability of organic matter rather than the specific bloom status. Overall, this research highlights the complex interactions governing marine ecosystems and highlights the importance of considering both biological and environmental factors in regulating marine ecosystem dynamics and productivity. Future studies should investigate trophic-level interactions across different ecological events to deepen our understanding of ecosystem resilience and response mechanisms.

CRediT authorship contribution statement

Yunjung Park: Writing – original draft, Visualization, Methodology, Formal analysis, Data curation. **Joonyeop Lee:** Writing – original draft, Visualization, Formal analysis, Data curation. **Soonmo An:** Writing – review & editing, Supervision, Project administration, Funding acquisition, Conceptualization. **Jaeho Cha:** Writing – review & editing, Supervision, Investigation, Conceptualization.

Declaration of generative AI and AI-assisted technologies in the writing process

During the preparation of this work the authors used ChatGPT in order to summarize highlights and improve overall readability. After using this tool, the authors reviewed and edited the content as needed and take full responsibility for the content of the publication.

Funding

This research was conducted within the project from the Korea Institute of Marine Science & Technology Promotion (KIMST), funded by the Ministry of Oceans and Fisheries (20220023).

Declaration of competing interest

The authors declare that they have no known competing financial interests or personal relationships that could have appeared to influence the work reported in this paper.

Acknowledgements

The authors thank to Yan Huang and Qinglong Zhang for their help.

Appendix A. Supplementary data

Supplementary data to this article can be found online at https://doi.org/10.1016/j.marenvres.2025.107553.

Data availability

The authors do not have permission to share data.

References

Agarwal, S., Dey, S., Ghosh, B., Biswas, M., Dasgupta, J., 2019. Mechanistic basis of vitamin B12 and cobinamide salvaging by the *Vibrio* species. Biochim. Biophys. Acta Proteins Proteom. 1867, 140–151.

Amin, S.A., Hmelo, L.R., van Tol, H.M., Durham, B.P., Carlson, L.T., Heal, K.R., Morales, R.L., Berthiaume, C.T., Parker, M.S., Djunaedi, B., Ingalls, A.E., Parsek, M.

R., Moran, M.A., Armbrust, E.V., 2015. Interaction and signaling between a cosmopolitan phytoplankton and associated bacteria. Nature 522, 98–101.
Anderson, S.R., Harvey, E.L., 2020. Temporal variability and ecological interactions of parasitic marine Syndiniales in coastal protest communities. mSphere 5, 209–220.
Antell, G.T., Saupe, E.E., 2021. Bottom-up controls, ecological revolutions and diversification in the oceans through time. Curr. Biol. 31, 1237–1251.
Azam, F., Fenchel, T., Field, J.G., Gray, J.S., Meyer-Reil, L.A., Thingstad, F., 1983. The ecological role of water-column microbes in the sea. Mar. Ecol. Prog. Ser. 10, 257–263.
Banse, K., 2007. Do we live in a largely top-down regulated world? J. Biosci. 32, 791–796.
Banse, K., 2013. Reflections about chance in my career, and on the top-down regulated world. Ann. Rev. Mar. Sci 5, 1–19.
Belfiore, A.P., Buley, R.P., Fernandez-Figueroa, E.G., Gladfelter, M.F., Wilson, A.E., 2021. Zooplankton as an alternative method for controlling phytoplankton in catfish pond aquaculture. Aquac. Rep. 21, 100897.
Buchan, A., LeCleir, G.R., Gulvik, C.A., Gonzalez, J.M., 2014. Master recyclers: features and functions of bacteria associated with phytoplankton blooms. Nat. Rev. Microbiol. 12, 686–698.
Calbet, A., Landry, M.R., 2004. Phytoplankton growth, microzooplankton grazing, and carbon cycling in marine systems. Limnol. Oceanogr. 49, 51–57.
Callahan, B.J., McMurdie, P.J., Rosen, M.J., Han, A.W., Johnson, A.J.A., Holmes, S.P., 2016. DADA2: high-resolution sample inference from Illumina amplicon data. Nat. Methods 13, 581–583.
Chen, X.-C., Kong, H.-N., He, S.-B., Wu, D.-Y., Li, C.-J., Huang, X.-C., 2009. Reducing harmful algae in raw water by light shading. Process Biochem. 44, 357–360.
Cho, D.-H., Ramanan, R., Heo, J., Lee, J., Kim, B.-H., Oh, H.-M., Kim, H.-S., 2015. Enhancing microalgal biomass productivity by engineering a microalgal-bacterial community. Bioresour. Technol. 175, 578–585.
Clavero, V., Izquierdo, J.J., Fernández, J.A., Niell, F.X., 2000. Seasonal fluxes of phosphate and ammonium across the sediment-water interface in a shallow small estuary (Palmones River, southern Spain). Mar. Ecol. Prog. Ser. 198, 51–60.
Costas-Selas, C., Martínez-García, S., Logares, R., Hernández-Ruiz, M., Teira, E., 2022. Role of bacterial community composition as a driver of the small-sized phytoplankton community structure in a productive coastal system. Microb. Ecol. 86, 777–794.
Cui, Y., Chun, S.-J., Baek, S.-S., Baek, S.H., Kim, P.-J., Son, M., Cho, K.H., Ahn, C.-Y., Oh, H.-M., 2020. Unique microbial module regulates the harmful algal bloom (*Cochlodinium polykrikoides*) and shifts the microbial community along the southern coast of Korea. Sci. Total Environ. 721, 137725.
Ekvall, M.K., Urrutia-Cordero, P., Hansson, L.-A., 2014. Linking cascading effect of fish predation and zooplankton grazing to reduced cyanobacterial biomass and toxin levels following biomanipulation. PLoS One 9, e112956.
Frank, K.T., Petrie, B., Shackell, N.L., 2007. The ups and downs of trophic control in continental shelf ecosystems. Trends Ecol. Evol. 22, 236–242.
Geng, H., Belas, R., 2010. Molecular mechanisms underlying roseobacter-phytoplankton symbioses. Curr. Opin. Biotechnol. 21, 332–338.
Goericke, R., 2002. Top-down control of phytoplankton biomass and community structure in the monsoonal Arabian Sea. Limnol. Oceanogr. 47, 1307–1323.
Gonzalez, L.E., Bashan, Y., 2000. Increased growth of the microalga *Chlorella vulgaris* when coimmobilized and cocultured in alginate beads with the plant-growth promoting bacterium *Azopirillum brasilense*. Appl. Environ. Microbiol. 66, 1527–1531.
Grattan, L.M., Holobaugh, S., Glenn Morris, J., 2016. Harmful algal blooms and public health. Harmful Algae 57, 2–8.
Hernandez, J.-P., de-Bashan, L.E., Rodriguez, D.J., Rodriguez, Y., Bashan, Y., 2009. Growth promotion of the freshwater microalga *Chlorella vulgaris* by the nitrogen-fixing, plant growth-promoting bacterium *Bacillus pumilus* from arid zone soils. Eur. J. Soil Biol. 45, 88–93.
Huys, R., Boxshall, G.A., 1991. Copepod Evolution the. Ray Society, London, p. 468.
Interlandi, S.J., Kilham, S.S., 2001. Limiting resources and the regulation of diversity in phytoplankton communities. Ecology 82, 1270–1282.
Issa, A.A., Abd-Alla, M.H., Ohyama, T., 2014. Nitrogen fixing cyanobacteria: future prospect. In: Ohyama, T. (Ed.), Advances in Biology and Ecology of Nitrogen Fixation. Tech Open Science, London, pp. 23–48.
Joglar, V., Álvarez-Salgado, X.A., Gago-Martinez, A., Leao, J.M., Pérez-Martínez, C., Pontiller, B., Lundin, D., Pihassi, J., Fernández, E., Teira, E., 2021. Cobalamin and microbial plankton dynamics along a coastal to offshore transect in the Eastern North Atlantic Ocean. Environ. Microbiol. 23, 1559–1583.
Kang, Y.S., Kwon, J.N., Shon, J.K., Hong, S.J., Kong, J.Y., 2003. Interrelation between water quality and community structure of phytoplankton around the season of red tide outbreak off the coast of Tongyeong area, 2002. J. Korean Fish. Soc. 36, 515–521.
Koch, F., Hattenrath-Lehmann, T.K., Goleski, J.A., Sañudo-Wilhelmy, S., Fisher, N.S., Gobler, C.J., 2012. Vitamin B1 and B12 uptake and cycling by plankton communities in coastal ecosystems. Front. Microbiol. 3, 363.
Kuhlisch, C., Shemi, A., Barak-Gavish, N., Schatz, D., Vardi, A., 2024. Algal blooms in the ocean: hot spots for chemically mediated microbial interactions. Nat. Rev. Microbiol. 22, 138–154.
Kujawinski, E.B., Longnecker, K., Barott, K.L., Weber, R.J.M., Soule, M.C.K., 2016. Microbial community structure affects marine dissolved organic matter composition. Front. Mar. Sci. 3, 45.
Lee, C.-H., Kang, M.-G., Lim, S.-Y., Kim, J.-H., Shin, J.-A., 2017. Environmental evaluation of fish aquafarm off Baegyado in Yeosu by multivariate analysis. J. Fish Mar. Sci. Educ. 29, 785–798.
Lee, M.-O., Kim, J.-K., 2008. Characteristics of algal blooms in the southern coastal waters of Korea. Mar. Environ. Res. 65, 128–147.
Levin, L.A., Ekau, W., Gooday, A.J., Jorissen, F., Middelburg, J.J., Naqvi, S.W.A., Neira, C., Rabalais, N.N., Zhang, J., 2009. Effects of natural and human-induced hypoxia on coastal benthos. Biogeosciences 6, 2063–2098.
Li, D., He, Y., Zheng, Y., Zhang, S., Zhang, H., Lin, L., Wang, D., 2022. Metaproteomics reveals unique metabolic niches of dominant bacterial groups in response to rapid regime shifts during a mixed dinoflagellate bloom. Sci. Total Environ. 823, 153557.
Liu, H., Buskey, E.J., 2000. The exopolymer secretions (EPS) layer surrounding *Aureoumbra lagunensis* cells affects growth, grazing and behavior of protozoa. Limnol. Oceanogr. 45, 1187–1191.
Metaxas, A., Scheibling, R.E., 1996. Top-down and bottom-up regulation of phytoplankton assemblages in tidepools. Mar. Ecol. Prog. Ser. 145, 161–177.
Miyoshi, S., 2013. Extracellular proteolytic enzymes produced by human pathogenic Vibrio species. Front. Microbiol. 4, 339.
Mitrovic, S.M., Chessman, B.C., Davie, A., Avery, E.L., Ryan, N., 2007. Development of blooms of Cyclotella Meneghiniana and Nitzschia Spp. (Bacillariophyceae) in a shallow river and estimation of effective suppression flows. Hydrobiologia 596, 173–185.
Morabito, G., Mazzocchi, M.G., Salmaso, N., Zingone, A., et al., 2018. Plankton dynamics across the freshwater, transitional and marine research sites of the LTER-Italy Network. Patterns, fluctuations, drivers. Sci. Total Environ. 627, 373–387.
Odate, T., Imai, K., 2003. Seasonal variation in chlorophyll-specific growth and microzooplankton grazing of phytoplankton in Japanese coastal water. J. Plankton Res. 25, 1497–1505.
Park, B.S., Kim, S., Kim, J.-H., Kim, J.H., Han, M.-S., 2019. Dynamics of *Amoebophyra* parasites during recurrent blooms of the ichthyotoxic dinoflagellate *Cochlodinum polykrikoides* in Korean coastal waters. Harmful Algae 84, 119–126.
Petrucciani, A., Chaerle, P., Norici, A., 2022. Diatoms versus copepods: could frustules traits have a role in avoiding predation? Front. Mar. Sci. 8, 804960.
Pruesse, E., Quast, C., Knittel, K., Fuchs, B.M., Ludwig, W., Peplies, J., Glöckner, F.O., 2007. SILVA: a comprehensive online resource for quality checked and aligned ribosomal RNA sequence data compatible with AR.B. Nucleic Acids Res. 35, 7188–7196.
R Core Team, 2016. R: A Language and Environment for Statistical Computing. R Foundation for statistical computing, Vienna, Austria.
Ramanan, R., Kim, B.-H., Cho, D.-H., Oh, H.-M., Kim, H.-S., 2016. Algae-bacteria interactions: evolution, ecology and emerging applications. Biotechnol. Adv. 34, 14–29.
Richlen, M., Morton, S.L., Jamali, E.A., Rajan, A., Anderson, D.M., 2010. The catastrophic 2008-2009 red tide in the Arabian Gulf region, with observations on the identification and phylogeny of the fish-killing dinoflagellate *Cochlodinium polykrikoides*. Harmful Algae 9, 163–172.
Riemann, L., Steward, G.F., Azam, F., 2000. Dynamics of bacterial community composition and activity during a mesocosm diatom bloom. Appl. Environ. Microbiol. 66, 578–587.
Rodríguez-Gálvez, S., Macías, D., Prieto, L., Ruiz, J., 2023. Top-down and bottom-up control of phytoplankton in a mid-latitude continental shelf ecosystem. Prog. Oceanogr. 217, 103083.
Saba, G.K., Steinberg, D.K., Bronk, D., 2009. Effects of diet on release of dissolved organic and inorganic nutrients by the copepod *Acartia tonsa*. Mar. Ecol. Prog. Ser. 386, 147–161.
Sailley, S.F., Polimene, L., Mitra, A., Atkinson, A., Allen, J.I., 2015. Impact of zooplankton food selectivity on plankton dynamics and nutrient cycling. J. Plankton Res. 37, 519–529.
Saito, H., Tsuda, A., Nojiri, Y., Nishioka, J., Takeda, S., Kiyosawa, H., Kudo, I., Noiri, Y., Ono, T., Taira, Y., Suzuki, K., Yoshimura, T., Boyd, P.W., 2006. Nutrient and phytoplankton dynamics during the stationary and declining phases of a phytoplankton bloom induced by iron-enrichment in the eastern subarctic Pacific. Deep-Sea Res, II: Top. Stud. Oceanogr. 53, 2168–2181.
Sin, Y., Lee, H., 2020. Changes in hydrology, water quality, and algal blooms in a freshwater system impounded with engineered structures in a temperate monsoon river estuary. J. Hydrol.: Reg. Stud. 32, 100744.
Sison-Mangus, M.P., Jiang, S., Kudela, R.M., Mehic, S., 2016. Phytoplankton-associated bacterial community composition and succession during toxic diatom bloom and non-bloom events. Front. Microbiol. 7, 1433.
Sommer, U., 2000. Scarcity of medium-sized phytoplankton in the northern Red Sea explained by strong bottom-up and weak top-down control. Mar. Ecol. Prog. Ser. 197, 19–25.
Stenseth, N.C., Llope, M., Anadón, R., Ciannelli, L., Chan, K.-S., Hjermann, D.Ø., Bagøien, E., Ottersen, G., 2006. Seasonal plankton dynamics along a cross-shelf gradient. Proc. R. Soc. B. Biol. Sci. 273, 2831–2838.
Strickland, J.D.H., Parsons, T.R., 1972. A Practical Handbook of Seawater Analysis. Fisheries Research Board of Canada, Ottawa.
Tilman, D., Kilham, S.S., Kilham, P., 1982. Phytoplankton community ecology: the role of limiting nutrients. Annu. Rev. Ecol. Systemat. 13, 349–372.
Van Dolah, F.M., 2000. Marine algal toxins: origins, health effects, and their increased occurrence. Environ. Health Perspect. 108, 133–141.
Van Kessel, M.A., Speth, D.R., Albertsen, M., Nielsen, P.H., Op den Camp, H.J.M., Kartal, B., Jetten, M.S.M., Lücker, S., 2015. Complete nitrification by a single microorganism. Nature 528, 555–559.

Vinueza, L.R., Menge, B.A., Ruiz, D., Palacios, D.M., 2014. Oceanographic and climatic variation drive top-down/bottom-up coupling in the Galápagos intertidal meta-ecosystem. Ecol. Monogr. 84, 411–434.
Zhang, Q., Warwick, R.M., McNeill, C.L., Widdicombe, C.E., Sheehan, A., Widdicombe, S., 2015. An unusually large phytoplankton spring bloom drives rapid changes in benthic diversity and ecosystem function. Prog. Oceanogr. 137, 533–545.
Zubkov, M.V., Fuchs, B.M., Tarran, G.A., Burkill, P.H., Amann, R., 2003. High rate of uptake of organic nitrogen compounds by *Prochlorococcus* cyanobacteria as a key to their dominance in oligotrophic oceanic waters. Appl. Environ. Microbiol. 69, 1299–1304.